

# Photoinduced Phase Transfer of Luminescent Quantum Dots to Polar and Aqueous Media

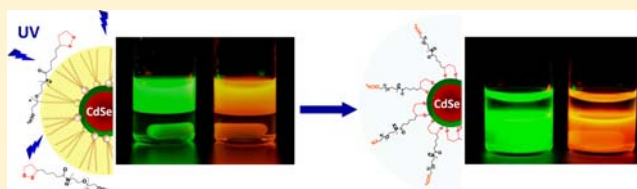
Goutam Palui,<sup>†</sup> Tommaso Avellini,<sup>†,§</sup> Naiqian Zhan,<sup>†</sup> Feng Pan,<sup>‡</sup> David Gray,<sup>‡</sup> Igor Alabugin,<sup>†</sup> and Hedi Mattoussi<sup>\*†</sup>

<sup>†</sup>Department of Chemistry and Biochemistry, Florida State University, 95 Chieftan Way, Tallahassee, Florida 32306, United States

<sup>‡</sup>Neuroscience Research Unit, Pfizer Global Research & Development, Eastern Point Road, Groton, Connecticut 06340, United States

**S** Supporting Information

**ABSTRACT:** We report a new strategy for the photo-mediated phase transfer of luminescent quantum dots, QDs, and potentially other inorganic nanocrystals, from hydrophobic to polar and hydrophilic media. In particular, we demonstrate that UV-irradiation ( $\lambda < 400$  nm) promotes the in situ ligand exchange on hydrophobic CdSe QDs with lipoic acid (LA)-based ligands and their facile QD transfer to polar solvents and to buffer media. This convenient method obviates the need to use highly reactive agents for chemical reduction of the dithiolane groups on the ligands. It maintains the optical and spectroscopic properties of the QDs, while providing high photoluminescence yield and robust colloidal stability in various biologically relevant conditions. Furthermore, development of this technique significantly simplifies the preparation and purification of QDs with sensitive functionalities. Application of these QDs to imaging the brain of live mice provides detailed information about the brain vasculature over the period of a few hours. This straightforward approach offers exciting possibilities for expanded functional compatibilities and reaction orthogonality on the surface of inorganic nanocrystals.



## INTRODUCTION

Fluorescent semiconductor nanocrystals (quantum dots, QDs) exhibit unique optical and spectroscopic properties that are not observed in their bulk parent materials or at the molecular scale.<sup>1–5</sup> Quantum dots made of CdSe, CdS, InAs, and InP cores have tunable size-dependent broad absorption, with high extinction coefficient, and size-dependent narrow Gaussian emission profiles.<sup>3,4,6,7</sup> CdSe-based nanocrystals, in particular, exhibit remarkable resistance to chemical and photodegradation and a high two-photon action cross section.<sup>3–5,8–11</sup> For a wide range of bioinspired applications, the optical and spectroscopic properties exhibited by luminescent QDs are unmatched by organic fluorophore and fluorescent proteins, which has spurred significant interest in developing QDs as fluorescent platforms and markers to increase our understanding of a variety of biological processes, ranging from sensing to the tracking of intracellular protein movements and interactions.<sup>8,10–18</sup> An important requirement for the effective integration into biotechnology is, however, the ability to access stable, water-soluble reagents that can be manipulated under a wide range of conditions (basic and acidic pHs, high concentrations of electrolytes and in the presence of reducing agents) and chemistries; the latter should allow straightforward and controllable coupling to various biomolecules.<sup>10,11,14,18,19</sup>

Highly luminescent QDs are reproducibly prepared with narrow size distribution and high fluorescence quantum yields by reacting organometallic precursors at high temperature in coordinating solutions.<sup>3,4,6,20–27</sup> These QDs are typically capped

with hydrophobic molecules (namely, trioctyl phosphine, TOP, trioctyl phosphine oxide, TOPO, along with alkylamines and phosphonic acid) and do not disperse in aqueous media. Postsynthetic surface modifications are thus required to render the QDs hydrophilic and biocompatible. An established strategy for preparing water-soluble QDs relies on replacing the native hydrophobic cap with bifunctional ligands that combine metal-chelating anchors onto the nanocrystal surfaces with hydrophilic modules that promote aqueous compatibility.<sup>28–34</sup> Two inherent properties of the ligands greatly influence the stability of the hydrophilic QDs: (1) the strength of the coordination binding between the anchoring groups and the inorganic surface; and (2) the affinity of the hydrophilic modules to buffer media.<sup>14,16–19</sup>

Ligands presenting multiple thiol anchoring groups, such as dihydrolipoic acid (DHLLA) in DHLLA-PEG and bis(DHLLA)-PEG, greatly enhance the QD stability over a wide range of biological conditions compared to monothiol-terminated ligands or other weakly coordinating groups.<sup>29–31,35,36</sup> The multiple contacts with the nanocrystal surface shifts the coordination equilibrium and decreases the dissociation rate of the multithiol ligands from the QD surfaces. Enhanced Au nanoparticle stability afforded by these multidentate ligands is also well documented.<sup>31,35,37–40</sup> However, reduction of the lipoic acid (LA) groups to DHLLAs is required for effective capping of QDs.<sup>28–31,35,36</sup> To date, the requisite reduced form of lipoic

Received: July 16, 2012

Published: August 31, 2012

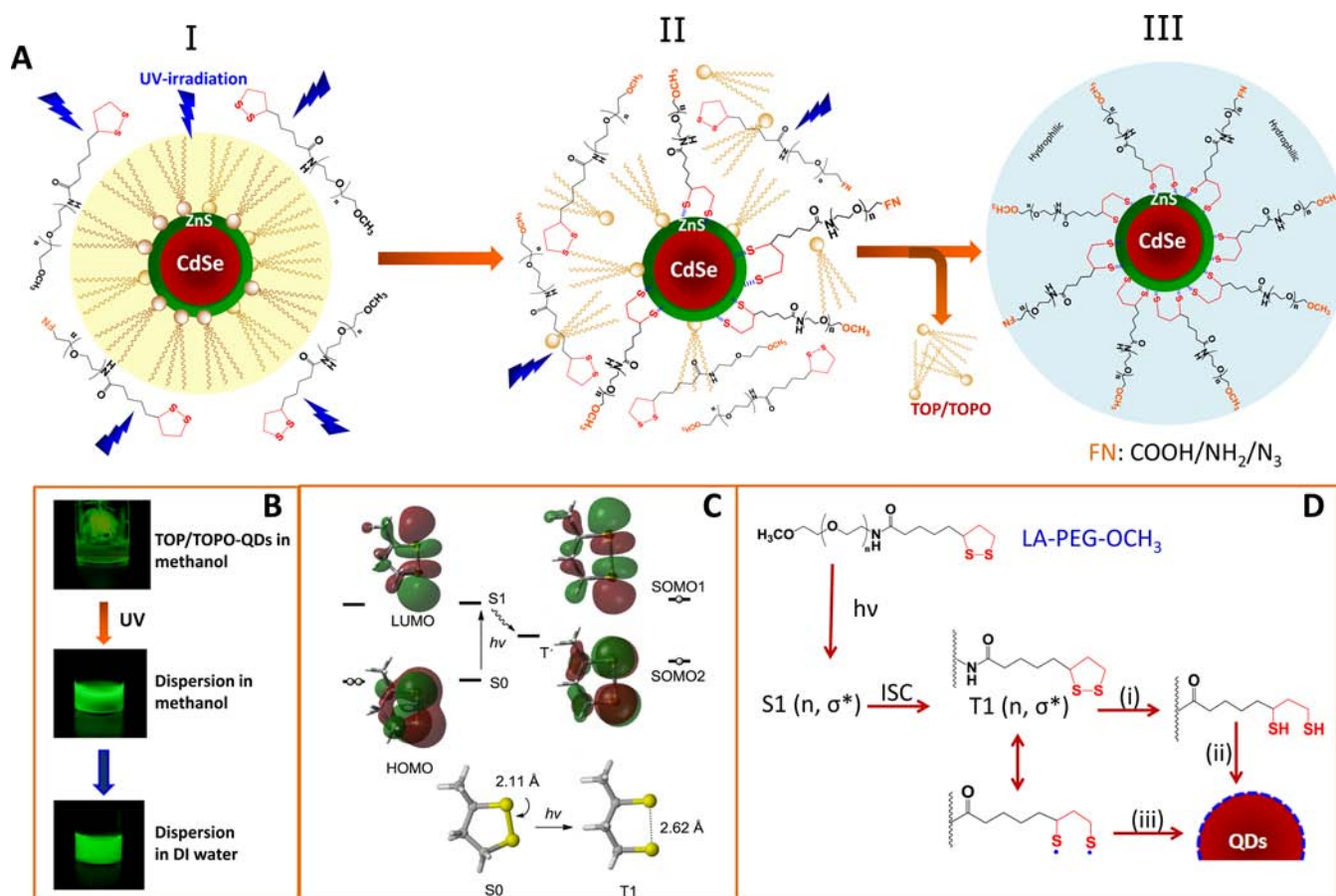


**Figure 1.** (A) Schematic depiction of the UV-promoted phase transfer of TOP/TOPO-QDs from hexane to methanol and other polar media including water; I and III designate the initial (hydrophobic) and final (hydrophilic) state of a QD, while II refers to an intermediate state where cap exchange is still incomplete. (B) Top vial shows QDs as wet paste (precipitated from hexane) mixed with methanol containing LA-PEG-OCH<sub>3</sub>; the system is heterogeneous. Middle and bottom vials show the dispersal of the same QDs upon UV-irradiation in methanol and their subsequent transfer to DI water. (C) Photochemical excitation of 3-alkyl-1,2-dithiacyclopentanes corresponds to the one-electron transfer from the Highest Occupied Molecular Orbital (HOMO) to the Lowest Unoccupied Molecular Orbital (LUMO). Subsequent Inter-System Crossing (ISC) transforms the initially formed S<sub>1</sub> state into the triplet state (T<sub>1</sub>) with the partially broken S-S bond. Molecular geometry and electronic structure were analyzed at the B3LYP/6-31+G(d,p) level of theory. (D) Schematic representation of the proposed mechanism(s) for the UV-induced transformation of the LA groups and ligand exchange on the QDs. Following UV excitation, the triplet state T<sub>1</sub>(n,σ\*) can produce either bond scission and dithiol formation (i) with subsequent ligand exchange on the QD (ii), or diradical formation followed by ligand exchange (iii). A list of ligands used with their chemical structures is provided in the Supporting Information.

acid used for the phase transfer has been prepared from dithiolane under strong reducing conditions using NaBH<sub>4</sub>.<sup>29,30,36,41,42</sup> While effective, this process imposes limitations with respect to the functional group tolerance and introduces an additional processing step with specific requirements. For instance, we found that NaBH<sub>4</sub>-reduction can alter the integrity of certain functional groups such as the terminal azide on LA-PEG-N<sub>3</sub>. This route also requires careful preparation, storage, and handling of the DHLA-based ligands under inert atmosphere to avoid reoxidation of the dithiol back to a disulfide.<sup>28,29,41</sup>

We were intrigued and inspired by a previous study by Sander and co-workers reporting that the cyclic disulfide core of lipoic acid has a well-defined absorption at ~350 nm and excitation at this wavelength produces a relatively long-lived ( $\tau \sim 0.1 \mu\text{s}$ ) triplet state, which can be converted into DHLA.<sup>43</sup> Even though the reported yields for this process were moderate, we anticipated that the presence of QDs could modulate the relative efficiency of the ring opening by intercepting the dithiol product due to the higher affinity of the bidentate ligands to the nanocrystal surfaces. We were further encouraged by the results

of our DFT calculations, which revealed that both the singlet (S<sub>1</sub>) and triplet (T<sub>1</sub>) excited states of LA correspond to n,σ\*-transitions which transfer electron density to the antibonding σ\*<sub>S-S</sub> orbital, thus significantly weakening the S-S bond (see Figure 1 and Supporting Information).<sup>44,45</sup> Together, these data suggested that the reduction of LA and concomitant cap-exchange can be promoted photochemically. Not only light is a green reagent with precisely controlled energy but it can also be delivered with high spatial and temporal selectivity.

In this report, we present a novel and operationally advantageous strategy for the photomediated transfer of ZnS-overcoated (e.g., CdSe core-plus-ZnS shell) QDs to buffer media. More precisely, we demonstrate that the oxidized lipoic acid (LA)-based ligands can be used “as is” (without prior reduction) to drive the cap exchange and QD transfer to polar organic solvents and buffer media, if aided with a UV irradiation (300 nm <  $\lambda$  < 400 nm). This process, which is applicable to several LA-based ligands, involves the photoinduced reduction of the LAs to DHLAs coupled with the simultaneous replacement of TOP/TOPO cap with the reduced ligands, all taking place in situ according to the general scheme outlined in Figure 1. Pure lipoic

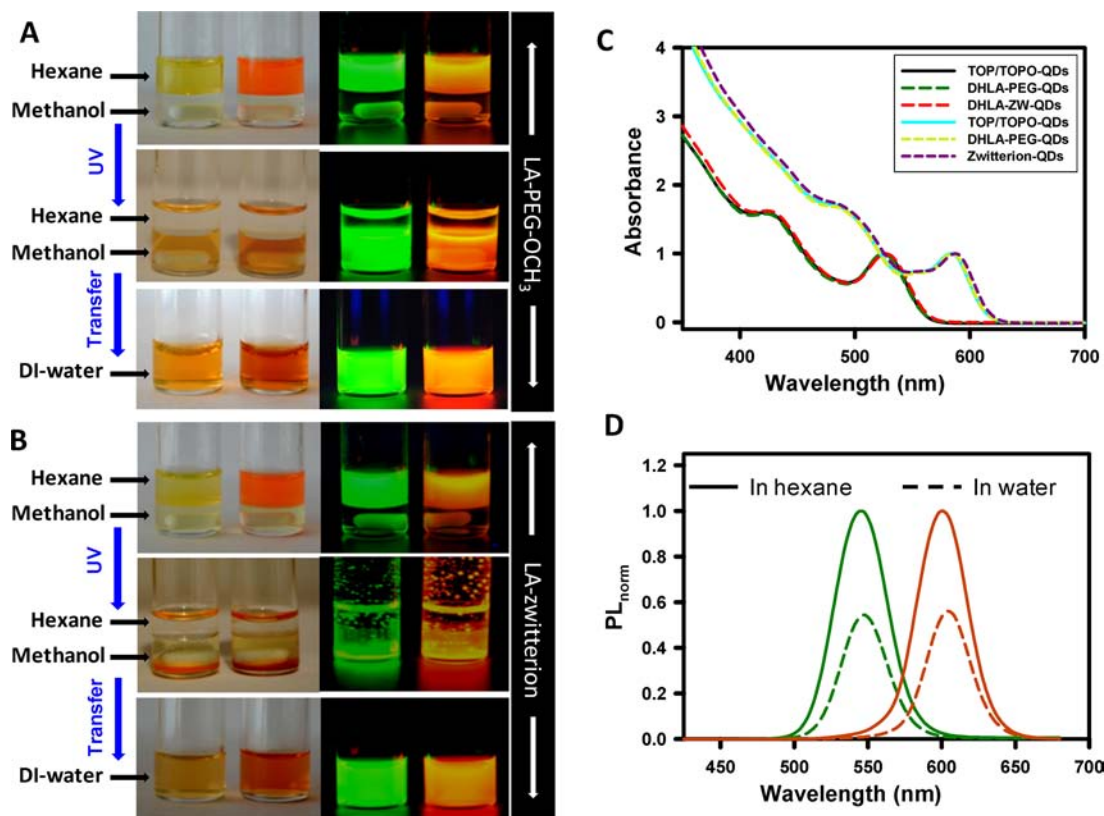


**Figure 2.** (A and B) Panels showing white light and fluorescent images (collected using hand-held UV lamp, with  $\lambda_{\text{exc}} = 365$  nm) of vials containing biphasic mixture of QDs in hexane (top phase) and LA-based ligand in methanol (bottom phase), before and after UV irradiation; (A) and (B) correspond to the procedures carried out using LA-PEG and LA-ZW ligands, respectively; the final QD dispersions in DI water are shown. (C) Normalized absorption spectra (with respect to the band edge peak) before and after phase transfer. (D) PL spectra of QDs in hexane and following phase transfer to water; spectra were normalized with the respect to peak value of TOP/TOPO-QDs. The PL spectra were collected from dispersions having the same optical density (O.D., i.e., same concentration) at the excitation line  $\lambda_{\text{exc}} = 350$  nm. Green and red lines correspond to the green and orange emitting QDs; the solid lines designate dispersions in hexane while dashed lines correspond to dispersions in DI water.

**Table 1. Characteristic Optical and Spectroscopic Data for QDs Dispersed in Water Following Transfer Using One Phase Route with Various Polar Solvents and in the Presence of LA-PEG-OCH<sub>3</sub>, or Transfer Using Two Phase Route in the Presence of LA-PEG-OCH<sub>3</sub> and LA-ZW Ligands<sup>a</sup>**

One Phase Route with LA-PEG-OCH <sub>3</sub>								
solvent	methanol	ethanol	1-propanol	2-propanol	1-butanol	<i>t</i> -butanol	DMF	acetonitrile <sup>b</sup>
Irradiation time (min)	20–25	20–30	15–20	100–120	90–100	20–30	55–65	90–100
Abs peak shift (nm)	No	2–3	No	No	No	4–5	2–3	2–3
PL peak shift (nm)	1–3	6–8	1–3	5–7	6–8	12–15	4–6	3–5
Two Phase Route with LA-PEG-OCH <sub>3</sub>			Two Phase Route with LA-ZW			Two Phase Route with LA		
solvent	methanol/hexane		methanol/hexane		methanol/DMF		methanol/hexane	
Irradiation time (min)	20–25		45–60		35–45		30–40	
Abs peak shift (nm)	No		No		No		1–2	
PL peak shift (nm)	1–3		No		No		1–3	

<sup>a</sup>This set of data is collected from 543 nm-emitting QDs. Similar data were measured from other nanocrystal dispersions. Overall, the PL quantum yield of the hydrophilic dispersions was consistently about 0.5–0.7 that of the native hydrophobic materials used, e.g., TOP/TOPO-QDs with a QY of 60% produced water-dispersion with ~30–35%. <sup>b</sup>Acetonitrile comparatively provides water dispersions of QDs with slightly lower PL yields.

acid (LA), LA-PEG-OCH<sub>3</sub>, LA-zwitterion (LA-ZW), and mixtures of LA-PEG-OCH<sub>3</sub> (or LA-ZW) and reactive LA-PEG-FN (with FN being COOH, NH<sub>2</sub>, or N<sub>3</sub>) have all been successfully used for this photochemically driven phase transfer. The in situ introduction of reactive groups onto the nanocrystal surface affords compatibility with commonly used conjugation techniques such as those based on carbodiimide chemistry. We will detail the steps involved and outline the relevant parameters that allow optimization of the phase transfer. Furthermore, we

exemplify the great performance of QD materials prepared in this fashion to the demanding application of *in vivo* imaging of the brain vasculature of live mice, where well-resolved vessel structures can be visualized for several hours using intravenously injected QDs, combined with two-photon fluorescence microscopy.

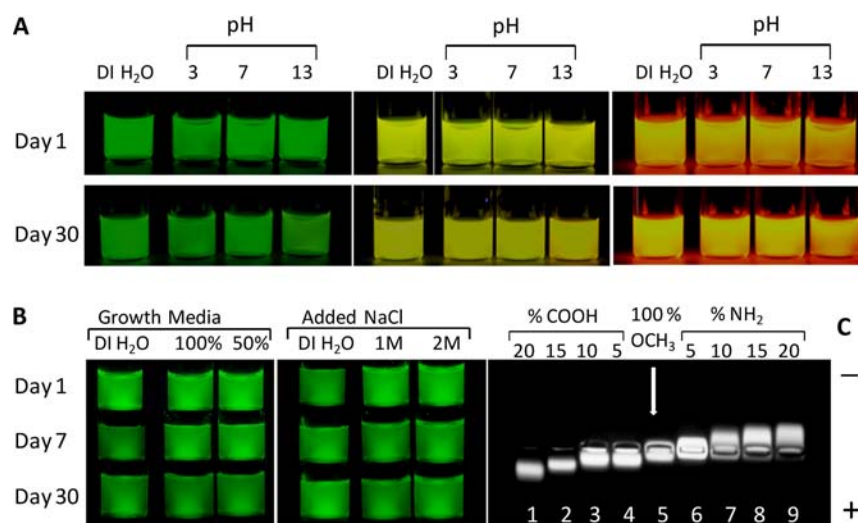


**Figure 3.** (A) Fluorescence images of vials containing green, yellow and orange-emitting QDs dispersed in PBS buffer (at  $1 \mu\text{M}$ ) at varying pH along with nanocrystals dispersed in DI water (control); QDs were phase-transferred via UV-irradiation in the presence of LA-PEG ligands. (B) Fluorescence images of vials containing green emitting QDs (at  $0.5 \mu\text{M}$ ) dispersed in growth media and in DI water with added 1 and 2 M NaCl. Images collected from freshly prepared samples are on top, images after several weeks of storage are shown below. The vials were illuminated with a hand-held UV lamp (excitation at 365 nm). (C) Gel electrophoresis image showing surface charge modulation in QDs phase-transferred with a mixture of LA-PEG-OCH<sub>3</sub>/LA-PEG-COOH or LA-PEG-OCH<sub>3</sub>/LA-PEG-NH<sub>2</sub> with increasing fraction of end-terminated ligands. Lanes 1–4 and 6–9 correspond to QD presenting LA-PEG-COOH and LA-PEG-NH<sub>2</sub>, respectively. A control dispersion of QD phase transferred with LA-PEG-OCH<sub>3</sub> is shown in lane 5.

## RESULTS AND DISCUSSION

The UV-promoted phase transfer can be carried out using two alternative procedures (see Figures 1 and 2). (1) In procedure 1, the hydrophobic QDs are first precipitated from nonpolar solvents as a “paste,” then mixed with a polar solvent containing LA-based ligands, and exposed to UV-light. (2) The second method involves irradiation of a biphasic mixture, with the nonpolar phase (e.g., hexane) containing the TOP/TOPO-capped QDs and the polar phase, that is immiscible with hexane (e.g., methanol and dimethylformamide, DMF), containing the LA-based ligands. In either procedure, the ligand exchange progressively alters the solubility of the native QDs, and promotes their transfer to the polar solvent(s).

While both methods allow the effective phase transfer of the nanocrystals to polar solvents and subsequently to water, each route offers certain advantages and flexibility. For example, route 1 allows the use of polar solvents with inherently distinct properties for the phase transfer, such as reducing capacity, polarity and boiling temperature. We have carried out the phase transfer using methanol, ethanol, 1-propanol, 2-propanol, 1-butanol, *tert*-butanol, DMF and acetonitrile (combined with LA-PEG ligands), with little variation in the quality of the final water-dispersed nanocrystals (see Table 1). In comparison, the two-phase reaction is much better suited (perhaps unique) when using LA-ZW, because of the stringent solubility requirements of this ligand; thus far, we found LA-ZW to be soluble in methanol, 1-propanol, DMF and water. Furthermore, because the light-induced ligand exchange with LA-ZW promotes nanocrystal precipitation, not only this approach provides a photochemical way to transfer QDs between solution and solid phases, it also allows a convenient means to purify the DHLA-ZW-capped QDs (these are not dispersible in either hexane or methanol). The only required operation is to remove the supernatant which contains excess ligands along with the released TOP/TOPO. Route 2 can be used with all LA-based ligands.

Having established that UV-irradiation could effectively replace the conventional multistep phase transfer of QDs using

$\text{NaBH}_4$ -reduced ligands, we tested whether this method has any effect on the optical and spectroscopic properties of the nanocrystals. We compared the absorption and PL spectra of various size QDs following the phase transfer mediated by LA-PEG-OCH<sub>3</sub> or LA-ZW ligands to those of the native TOP/TOPO-QDs, and found that the spectroscopic properties were essentially unchanged. Figure 2 shows the absorption and PL spectra of green- and orange-emitting CdSe-ZnS QDs, dispersed in hexane (TOP/TOPO-capped) and in DI water (capped with photogenerated LA-PEG-OCH<sub>3</sub>). Similar optical data were collected from other (blue-, yellow- and red-emitting) QDs, and with other LA-based ligands. Initially, a slight (4–7 nm) emission red shift was occasionally observed for dispersions prepared using LA-PEG ligands and  $\sim 45$ –60 min UV-irradiation time (data not shown). Similarly, a slight red shift can be measured for dispersions prepared using the conventional route with borohydride-reduced ligands.<sup>31</sup> Upon further exploration, we found that addition of a small amount of tetramethyl ammonium hydroxide (TMAH) prior to the cap exchange, shortened the necessary irradiation time for a full phase transfer to 20–25 min, and produced water dispersions that exhibited negligible red shift in the PL peak location (e.g., 1–3 nm shift with 1-propanol and methanol, see Table 1). Transfer of nanocrystals in the presence of LA-ZW required longer irradiation time ( $\sim 45$ –60 min), while producing hydrophilic QDs with PL and absorption peak positions that were essentially identical to those of the starting hydrophobic materials (see Table 1).

This strategy allowed us to introduce functional/reactive groups on the surface of the hydrophilic nanocrystals by comixing a varying molar fraction of LA-PEG-FN ligands (e.g., LA-PEG-NH<sub>2</sub> or LA-PEG-COOH) with respect to the total amount of ligands prior to UV treatment. Indeed, this method produces hydrophilic QDs with a statistical distribution of the desired functional groups on their surfaces, as shown by the gel electrophoresis panel in Figure 3. The sign and magnitude of the mobility shift depend on the nature of the groups introduced (e.g., amine versus carboxy) and on the molar fraction used, with

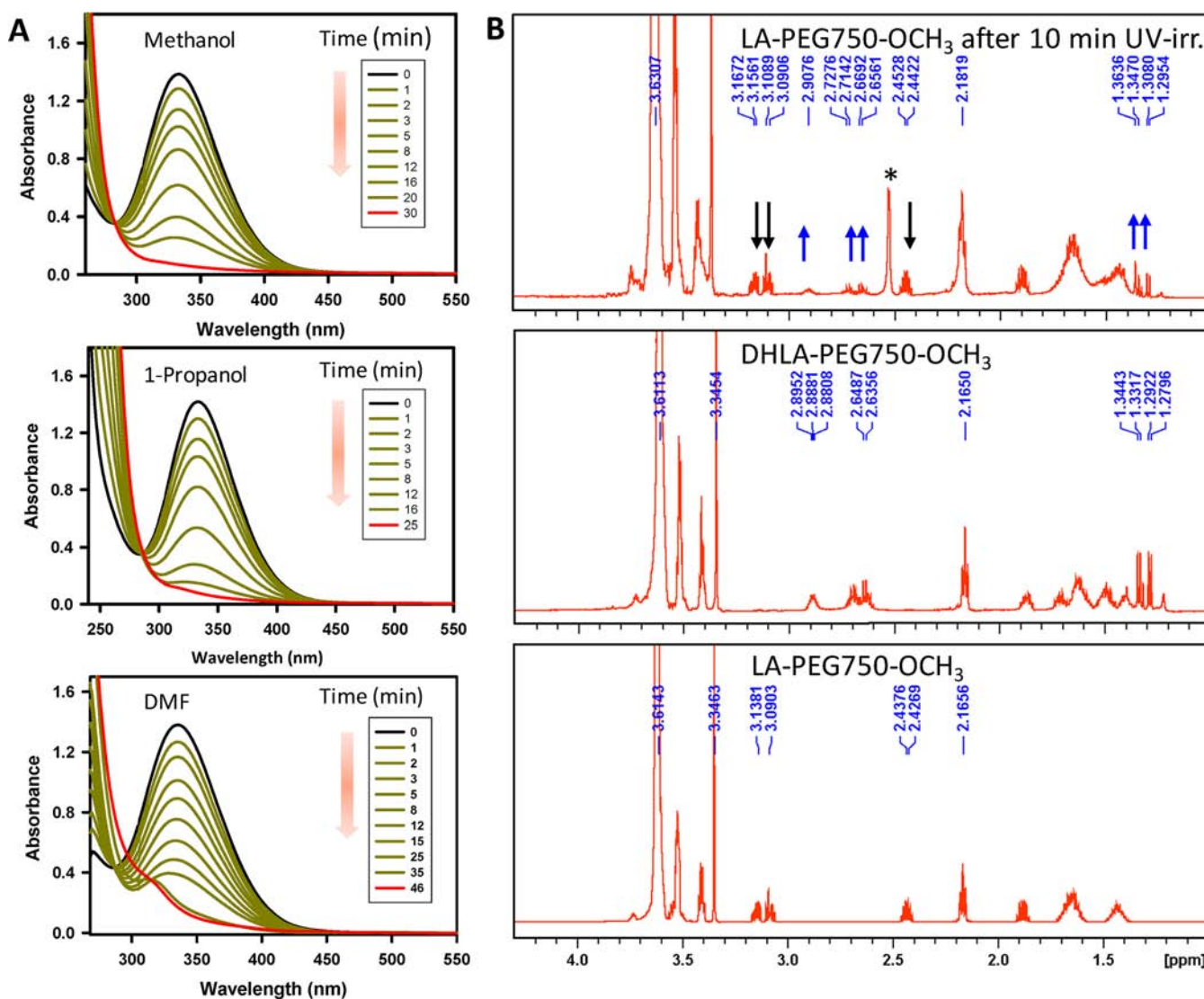


**Figure 4.** (A) Progression of the UV absorption spectra of LA-PEG750-OCH<sub>3</sub> dissolved in methanol, 1-propanol and DMF, respectively, collected after irradiation times varying from 1 to 30 min; ligand concentration was  $\sim 10$  mM. (B) <sup>1</sup>H NMR spectra collected from LA-PEG750-OCH<sub>3</sub> (bottom), NaBH<sub>4</sub>-reduced LA-PEG750-OCH<sub>3</sub> (center) and LA-PEG750-OCH<sub>3</sub> following UV irradiation for 10 min in methanol (top); a mixture of oxidized (LA with peaks at 2.4 and 3.0–3.1 ppm) and reduced (DHLA with peaks at 1.29 and 1.36 ppm attributed to thiols) terminal groups are present. All spectra were collected from ligand dissolved in CDCl<sub>3</sub>. The peak at  $\sim 2.5$  designated by \* comes from impurities.

larger mobility shifts measured for higher fractions of end-functionalized ligands.<sup>31</sup> Additional proofs for the introduction of functional groups onto the QD surfaces are provided by FT-IR spectroscopy (e.g., for FN=N<sub>3</sub> see Supporting Information).

The quantum yield measurements revealed that the photo-mediated cap exchange reliably produces materials which exhibit comparable or slightly higher PL quantum yields than those transferred using NaBH<sub>4</sub>-reduced ligands. The PL quantum yields (QYs) measured for the present hydrophilic QDs are smaller than those measured for the native hydrophobic materials, which is consistent with the literature data for thiol-based ligand exchange (QY of DHLA-PEG-QDs  $\sim 50$ –70% of that measured for TOP/TOPO-QDs).<sup>28,30,35,36</sup>

Colloidal stability is a critically important property of hydrophilic nanocrystalline materials. We investigated the aggregation propensity of QD dispersions prepared using our new procedure relative to those produced with NaBH<sub>4</sub>-reduced ligands. Figure 3 shows images of several dispersions of green-, yellow- and orange-emitting QDs in buffers with pH ranging

from 3 to 13 immediately following transfer and after several weeks of storage, side-by-side with dispersions in DI water. Figure 3 also shows images of the same QD dispersions containing excess electrolytes (1 and 2 M NaCl) and in cell growth media, freshly prepared and after several weeks of storage. Additional stability tests on these QDs, along with a comparison to those prepared using the conventional procedure, are provided in the Supporting Information. These images demonstrate that the UV-promoted ligand exchange can be used to access materials that are on par with, or even better than those prepared using the conventional route and DHLA-based ligands. In actual practice, the QD dispersions are colloidal stable for at least several months of storage.<sup>29,31</sup>

Further examining the scope of the UV-promoted phase transfer we found that this approach can be directly applied to core only CdSe QDs, albeit with a near complete loss in the QD photoemission. Moreover, we have found that this strategy can be easily applied to gold nanoparticles, and we anticipate that it would potentially be applicable to a whole range of other

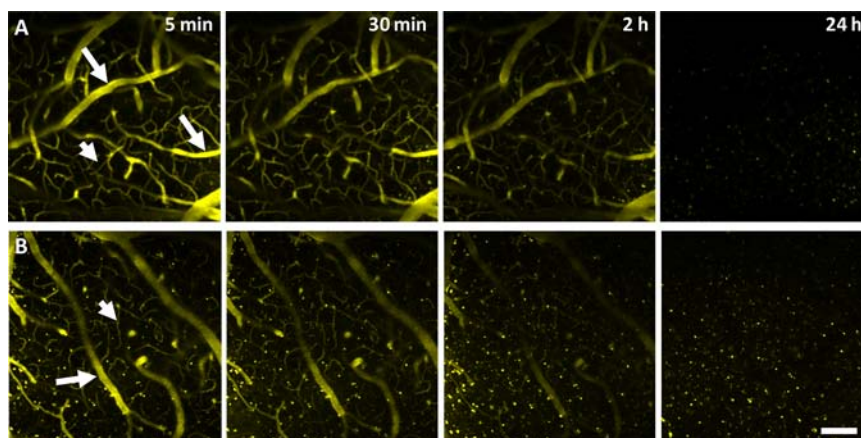


**Figure 5.** Images of the vasculature of cerebral cortex collected from two separate animals, microinjected with QDs phase transferred with LA-PEG750-OCH<sub>3</sub> ligands (A), or with QDs phase transferred using LA-ZW ligands (B). The panels in each row correspond to images collected after a given time lapse following QD delivery. The well-resolved structures of the arteriolo/venule (arrow) and capillaries (arrowhead) are detected at a depth within 200  $\mu\text{m}$  below the cranial window. No QD aggregation was detected in the cortical vasculature during the imaging time span. Nor did we detect obvious penetration of QD through blood–brain barrier. QD signal progressively decreases with time before reaching background levels at 24 h. Scale bar: 100  $\mu\text{m}$ . The bright spots present in all the panels correspond to autofluorescence signal generated from the brain macrophage, which density depends on the age of the animal used.

nanoparticles. The results and details of these ongoing studies will be reported in due course.

**Proposed Mechanism.** Our data on the ligand exchange can be combined to develop a mechanistic insight into the phase transfer of the nanocrystals. We found that irradiation in the UV range ( $300 < \lambda < 400 \text{ nm}$ ) is a prerequisite for a successful and effective phase transfer of the QDs. Irradiation in the “visible” leads to incomplete phase transfer and afforded only QDs with poor stability, and extending the irradiation time did not lead to improved yields or nanocrystal quality. With the materials and size regime investigated in this study, UV-promoted transfer requires an optical irradiation for 20–60 min (at  $4.5 \text{ mW/cm}^2$ ), with the exact time depending on the QD concentration, nature of the ligands and solvents; higher concentrations of QDs require longer irradiation times. Rapid and complete phase transfer generally requires a large excess of LA-based ligands with respect to the QD concentration ( $\sim 10\,000$  times excess). However, we found that holding other reaction variables constant (same DHLA-PEG ligand, solvent, TOPO-capped QD, reaction time, and QD concentration), complete UV-facilitated phase transfer was achieved with concentrations of LA-PEG ligands about one-half of what was required for the conventional phase transfer process. To investigate the effect of UV-irradiation on the ligands, a series of control experiments were conducted wherein solutions of the ligands were loaded in a 1 cm quartz cuvette and irradiated without addition of QD materials. Under these conditions, irradiation produced a progressive reduction in the absorption peak centered at  $\sim 340 \text{ nm}$  (signature of the LA group) with time, with a near complete disappearance of that peak after 25–30 min (see Figure 4). Similar observations have been reported for UV-irradiated pure lipoic acid in polar solvents, see Supporting Information and reference.<sup>43</sup> UV-induced transformation of the ligand can be effectively accomplished in a variety of solvents, including polar protic solvents (e.g., methanol and 1-propanol) and aprotic solvents (e.g., DMF and acetonitrile). However, irradiation of the ligand dispersed in non polar, or hydrogen-depleted solvents produced a much slower progression in the UV absorption (peak at  $\sim 340 \text{ nm}$ ) without reaching saturation.

Additional evidence that progressive transformation of the disulfide groups to dithiols takes place, even in the absence of QDs, comes from <sup>1</sup>H NMR experiments on the ligands following UV-irradiation. This transformation is reflected in the appearance of characteristic DHLA NMR signals such as triplet and doublet at 1.35 and 1.30 ppm (for the SH group at a primary and secondary carbons, respectively), and the multiplets at 2.9 and 2.7 ppm gradually replacing the LA resonances (see Figure 4). The new set of NMR peaks is identical to the key NMR signals of NaBH<sub>4</sub>-reduced LA.<sup>29,36</sup> This molecular-level chemistry associated with photoinduced reduction of the LA-containing ligands will be investigated in future studies.

Taken together, the above results suggest that ligands undergo UV-induced reduction of the disulfide ring, a process that is potentially accelerated when irradiation occurs in the presence of QDs. We found that the photoreduction can be exploited to streamline the preparation of pure and stable QDs with water solubilizing LA ligands. When QDs are present in the medium they can serve two facilitating roles: (1) acting as photosensitizers, providing excited electrons to enhance the reduction of the ligands, though this process may be rather modest because the oxidized ligands are not bound to the nanocrystal surfaces;<sup>46,47</sup> (2) providing a sink for reaction products by virtue of the preferential binding of reduced LAs to the QD surface. The photoinduced electron transfer requires close proximity between the LA groups and the nanocrystal surfaces protected by the TOP/TOPO ligands. Because the QD photoexcitation contribution to the overall ligand reduction is further decreased by the relatively low concentration of both reagents in these experiments ( $\sim 100 \text{ mM}$  ligands and  $\sim 1.5\text{--}2.5 \mu\text{M}$  QDs), coupling of the reduction process with cap exchange on TOP/TOPO-QDs is likely to play an important role in driving the phase transfer reaction to completion.

**Fluorescence Imaging of the Brain Vasculature of Live Mice.** Optical reagents find numerous applications in the study of biological processes in vitro and in vivo. In general, useful labels must combine several features suitable for the targeted experiment, including optical properties (QY, specific excitation and emission spectra, photostability), physical properties (size, charge, chemical and colloidal stability), and biological properties

(stability toward aggregation and metabolic degradation, desired tissue partitioning, and lack of toxicity). For example, live animal imaging has demanding requirements for the fluorophore performance and stability. Ideally, a fluorescent marker will have high QY, a tunable emission spectrum, good stability toward both degradation and elimination over several hours, well-defined intrinsic partitioning into a particular organ, tissue, or cell type, and should be amenable to functionalization using facile and diverse chemistries. Among several investigations into the utility of QDs prepared via UV-induced phase transfer, we examined the performance of these reagents, including their brightness, biostability, and their potential effects on the physiological microenvironment by imaging the integrity of QD-labeled brain microvasculature over a 24 h period in live mice. For this specific application, in addition to the above requirements a chromophore must also have limited intrinsic partitioning into brain tissue, must be small enough to enter brain microcapillaries, and must not disrupt the integrity of the blood-brain barrier. Previous studies showed that CdSe-ZnS QDs are excellent *in vivo* imaging reagents because they exhibit very large two-photon absorption cross section, with values as high as 47 000 Goepfert-Mayer units; these are about 2–3 orders of magnitude higher than those of conventional dyes and fluorescent proteins.<sup>8,9,48</sup> Furthermore, Webb and co-workers showed that combined with the use of NIR irradiation two-photon fluorescence using QDs could allow deep tissue imaging with reduced background contributions.<sup>8</sup>

We performed two-photon fluorescence imaging of the brain vessels (including capillaries) of live mice using QDs phase-transferred in the presence of LA-PEG-OCH<sub>3</sub> or LA-ZW ligands. Thinned skull cranial window surgery is a minimally invasive procedure to image various cellular and tissue structures of a rodent brain.<sup>49,50</sup> 6–7 month C57BL6 mice were first anesthetized with ketamine and xylazine (80 mg/kg ketamine, 12 mg/kg xylazine). A ~500  $\mu\text{m}$  region over the somatosensory cortex were thinned to ~20  $\mu\text{m}$ . Following surgery the animals were intravenously injected with 20–50  $\mu\text{L}$  of QDs (3–6  $\mu\text{M}$ ) dispersed in PBS buffer and targeting an initial concentration of ~0.1  $\mu\text{M}$  in blood. The first set of images was acquired 5 min after injection, followed by additional ones collected after 30 min, 2 and 24 h.

The collected fluorescence images show well resolved capillary structures with a submicrometer resolution (see Figure 5). The vasculature could be effectively imaged up to ~200  $\mu\text{m}$  deep (from the surface). Significantly, the QDs remained visible in the blood circulation for up to 2 h without any visible self-aggregation or blockage of the microcapillaries. The signal decreased to background levels by 24 h, which suggests that these QDs do not inherently partition into brain tissue or endothelial cells, and were progressively cleared from the blood circulation, likely due to renal filtration.<sup>51</sup> Indeed, we observed increased fluorescence in mouse urine 2 h after injection. We should emphasize that the ability to image the blood brain capillary for such extended period of time constitutes a very promising capability, as it permits one to investigate the structure and integrity of the blood capillaries in the brain of live animals under different conditions. With vascularly restricted molecular scale fluorophores such as Cascade Blue dextran or 4k dextran conjugated FITC, useful signal is detected only for a few minutes, due to combination of accelerated photobleaching of the dye and rapid clearance.<sup>52</sup> By comparison, these hydrophilic QDs provide a high signal-to-noise ratio, and due to a combination of their nanometer size and relatively inert coating, have significantly

extended circulating half-life, allowing effective imaging of the capillaries over several hours. It is also worth noting that the concentration of QDs used in this study to label the brain vessel is only ~10% of that used in previous work to image skin capillaries,<sup>8</sup> further confirming the great utility of these specific QDs to label even the finest vessels (structure <10  $\mu\text{m}$  in diameter, see Figure 5).

## CONCLUSION

We have developed a new strategy to promote the transfer of luminescent QDs (and potentially other inorganic nanocrystals) to polar solvents and buffers mediated by UV-irradiation. This strategy provides highly luminescent hydrophilic QDs of various sizes that show remarkable colloidal stability and maintain the original optical and spectroscopic properties of their hydrophobic counterparts. The flexibility of this strategy is illustrated by the preparation of hydrophilic nanocrystals with controllable nature and density of reactive functionalities. This approach presents a range of exciting possibilities for expanded functional group compatibilities and orthogonal reactivities on the nanocrystal surfaces. For instance, it has allowed the preparation of quantum dots surface-functionalized with azide groups, which potentially permit the use of chemical coupling based on copper-free strain-promoted azide–alkyne cycloaddition (SPAAC) directly onto the nanocrystals. Chemical reduction of the disulfide ring using borohydride alters the integrity of some sensitive reactive groups, such as azide and aldehyde, rendering the preparation of azide- and aldehyde-functionalized nanocrystals (via DHLA-PEG route) essentially impossible. The procedure is simple to implement, effective, and has the potential to be extended to a variety of inorganic nanocrystals. We have further demonstrated the utility and stability of QDs prepared via this approach in a demanding *in vivo* application where they were used to effectively visualize the brain capillaries of live mice for several hours without apparent adverse effects. Our work may lead to a broad spectrum of studies which apply functionally modified QDs to a variety of biological systems, from cultured cells to intact organisms.

## EXPERIMENTAL SECTION

**Methods.** Detailed information about the ligand synthesis and characterization can be found in previous reports.<sup>29,32,53</sup> The QDs we used in this study are CdSe-ZnS core–shell prepared stepwise using reduction of organometallic precursors at high temperature following the synthetic rationales described in previous reports.<sup>6,21,23,24,27,28,54</sup> Below we briefly describe the experimental procedure used for the transfer of QDs using the “one phase reaction” (route 1) in the presence of LA and LA-PEG, or the “two phase reaction” (route 2) in the presence of LA, LA-PEG, and LA-ZW.

**Transfer of Quantum Dots Using One-Phase Reaction and LA-Based Ligands.** In a glass vial, 100  $\mu\text{L}$  of 15–20  $\mu\text{M}$  stock solution (~1.5–2.0 nmol) of CdSe-ZnS QDs was precipitated with ethanol (two rounds) and mixed as a paste with 1.5 mL of methanol or 1-propanol containing LA-PEG (0.03–0.1M) and TMAH (~5 mM). A magnetic stirring bar was introduced, the vial was sealed with a rubber septum, and the atmosphere was switched to nitrogen by applying 3 to 4 rounds of mild vacuum followed by flushing with nitrogen. The vial was then placed in the UV reactor (Model LZC-4 V, Luzchem Research, Inc., Ottawa, Canada) and irradiated for 20 min ( $\lambda_{\text{irr}}$  maximum peak at 350 nm, 4.5 mW/cm<sup>2</sup>) with vigorous stirring, resulting in a homogeneous QD dispersion in the polar solvent. The solvent was removed under vacuum, followed by redispersion of the QDs in an ethanol/chloroform mixture. Then, hexane was slowly added (hexane/ethanol/chloroform = 20:10:1) to precipitate out the QDs. Following centrifugation, the supernatant was removed, the content was mildly dried under vacuum

for ~5 min, and buffer was added to disperse the QDs. This aqueous dispersion of QDs was filtered through 0.45  $\mu\text{m}$  syringe filter and further purified by applying 1–2 rounds of concentration/dilution using a membrane filtration device Amicon Ultra 50,000 MW (from Millipore) to remove excess ligands and solubilized TOP/TOPO. The concentrated QDs were finally dispersed in DI water or buffers at a concentration of 5–10  $\mu\text{M}$  (stock solution) and stored in the refrigerator at 4  $^{\circ}\text{C}$  for later use. We should note that shorter wavelength irradiation (at 300–313 nm) can be used. However, this UV range is overall less effective and it requires that materials be loaded into a quartz vial where light absorption by the cell walls is negligible compared to that exhibited by scintillation vials.

**Transfer of QDs Using Two-Phase Reaction.** In a typical reaction, 100  $\mu\text{L}$  of 15–20  $\mu\text{M}$  stock solution (~1.5–2.0 nmol) of CdSe-ZnS QDs were precipitated with ethanol (two rounds), then dispersed in 750  $\mu\text{L}$  of *n*-hexane (in a glass vial). A total of 500  $\mu\text{L}$  of methanol containing pure LA-PEG-OCH<sub>3</sub>, or a mixture of LA-PEG-OCH<sub>3</sub> and LA-PEG-FN (~100 mM) and TMAH (10 mM) was added. A magnetic stirring bar was inserted, the vial was sealed with a rubber septum, and the atmosphere was switched to nitrogen by applying 3 to 4 rounds of mild vacuum followed by flushing with nitrogen. The vial was placed in the UV reactor, irradiated for 20 min, and then retrieved for further processing. Following irradiation, observation under white light showed that the top hexane layer became completely transparent while the bottom methanol layer became colored, indicating transfer of the QD material to methanol (Figure 2, main text). When observed under hand-held UV lamp, the fluorescence signal was initially limited to the hexane layer, but after photoreduction, the signal exclusively emanated from the methanol layer (Figure 2, main text). The organic solvents (hexane and methanol) were removed under vacuum, and the QDs were transferred to buffer following the same steps (precipitation, centrifugation and purification using a filtration device) as described above. When the above procedure was applied to TOP/TOPO-QDs in the presence of LA-ZW, an additional benefit of the phase transfer can be realized. Though DHLA-ZW and LA-ZW were fully dispersible in methanol and DMF, DHLA-ZW-capped QDs were not. This produced precipitation of the DHLA-ZW-QDs while free ligands stayed dispersed in the solvent.

Transfer of QDs using pure lipoic acid can be carried using either route, with a slight modification. Following UV-irradiation, the slightly turbid dispersion of QDs in the polar phase (methanol) was dried under vacuum. Hexane was added to the precipitate, and the mixture was centrifuged to remove the solubilized TOP/TOPO. The solvent was decanted and water mixed with potassium-*tert*-butoxide (*K-t-B*, 1.5 equiv with respect to the initial amount of LA ligand) was added, resulting in a clear QD dispersion. Here *K-t-B* was needed to shift the equilibrium of the medium to basic pH where the carboxy groups are deprotonated.<sup>28</sup>

**Fluorescence Imaging of the Brain Blood Capillaries of Live Animals.** Fluorescence images of the blood vasculature through a thinned skull window were acquired using an Olympus Fluoview FV1000MPE multiphoton laser-scanning microscope. A mode-locked DeepSee Mai Tai Ti:sapphire laser (Mai Tai; Spectra-Physics) emitting at 840 nm was used for excitation; the excitation power at the sample was 15–40 mW. Fluorescence signal from the specimen was collected using a 20 $\times$  water immersion objective (Olympus, N/A = 1.00) and the photons within 575–630 nm range were selected via an Olympus filter set and detected by a Hamamatsu photomultiplier tube.

## ■ ASSOCIATED CONTENT

### ● Supporting Information

Information on DFT calculation of the photochemical excitation of lipoic acid, additional experimental details on the phase transfer, the ligand structure, colloidal stability of the QD dispersions, UV-vis Abs data of the ligands as function of the UV-irradiation times and in various solvents, and FT-IR data. This material is available free of charge via the Internet at <http://pubs.acs.org>.

## ■ AUTHOR INFORMATION

### Corresponding Author

mattoussi@chem.fsu.edu

### Present Address

<sup>§</sup>University of Bologna, Department of Chemistry, via Selmi 2, 40126 Bologna, Italy

### Notes

The authors declare no competing financial interest.

## ■ ACKNOWLEDGMENTS

The authors thank FSU and the National Science Foundation for financial support: NSF-CHE, Grants Nos. 1058957 (H.M.) and 1213578 (I.A.). The authors also thank Xin Ji and H. B. Na for the helpful discussions. We also thank Lei Bruscheiler for assistance with the gel experiments.

## ■ REFERENCES

- (1) Brus, L. *J. Phys. Chem.* **1986**, *90*, 2555.
- (2) Alivisatos, A. P. *Science* **1996**, *271*, 933.
- (3) Murray, C. B.; Kagan, C. R.; Bawendi, M. G. *Annu. Rev. Mater. Sci.* **2000**, *30*, 545.
- (4) Talapin, D. V.; Lee, J. S.; Kovalenko, M. V.; Shevchenko, E. V. *Chem. Rev.* **2010**, *110*, 389.
- (5) Vanmaekelbergh, D. *Nano Today* **2011**, *6*, 419.
- (6) Murray, C. B.; Norris, D. J.; Bawendi, M. G. *J. Am. Chem. Soc.* **1993**, *115*, 8706.
- (7) Guzelian, A. A.; Banin, U.; Kadavanich, A. V.; Peng, X.; Alivisatos, A. P. *Appl. Phys. Lett.* **1996**, *69*, 1432.
- (8) Larson, D. R.; Zipfel, W. R.; Williams, R. M.; Clark, S. W.; Bruchez, M. P.; Wise, F. W.; Webb, W. W. *Science* **2003**, *300*, 1434.
- (9) Clapp, A. R.; Pons, T.; Medintz, I. L.; Delehanty, J. B.; Melinger, J. S.; Tiefenbrunn, T.; Dawson, P. E.; Fisher, B. R.; O'Rourke, B.; Mattoussi, H. *Adv. Mater.* **2007**, *19*, 1921.
- (10) Jaiswal, J. K.; Mattoussi, H.; Mauro, J. M.; Simon, S. M. *Nat. Biotechnol.* **2003**, *21*, 47.
- (11) Wu, X. Y.; Liu, H. J.; Liu, J. Q.; Haley, K. N.; Treadway, J. A.; Larson, J. P.; Ge, N. F.; Peale, F.; Bruchez, M. P. *Nat. Biotechnol.* **2003**, *21*, 41.
- (12) Bruchez, M.; Moronne, M.; Gin, P.; Weiss, S.; Alivisatos, A. P. *Science* **1998**, *281*, 2013.
- (13) Chan, W. C. W.; Nie, S. M. *Science* **1998**, *281*, 2016.
- (14) Medintz, I. L.; Uyeda, H. T.; Goldman, E. R.; Mattoussi, H. *Nat. Mater.* **2005**, *4*, 435.
- (15) Biju, V.; Itoh, T.; Ishikawa, M. *Chem. Soc. Rev.* **2010**, *39*, 3031.
- (16) Zrazhevskiy, P.; Sena, M.; Gao, X. H. *Chem. Soc. Rev.* **2010**, *39*, 4326.
- (17) Sperling, R. A.; Parak, W. *Philos. Trans. R. Soc., A* **2010**, *368*, 1333.
- (18) Michalet, X.; Pinaud, F. F.; Bentolila, L. A.; Tsay, J. M.; Doose, S.; Li, J. J.; Sundaresan, G.; Wu, A. M.; Gambhir, S. S.; Weiss, S. *Science* **2005**, *307*, 538.
- (19) Janczewski, D.; Tomczak, N.; Han, M. Y.; Vancso, G. J. *Nat. Protoc.* **2011**, *6*, 1546.
- (20) Peng, X. G.; Schlamp, M. C.; Kadavanich, A. V.; Alivisatos, A. P. *J. Am. Chem. Soc.* **1997**, *119*, 7019.
- (21) Dabbousi, B. O.; RodriguezViejo, J.; Mikulec, F. V.; Heine, J. R.; Mattoussi, H.; Ober, R.; Jensen, K. F.; Bawendi, M. G. *J. Phys. Chem. B* **1997**, *101*, 9463.
- (22) Peng, Z. A.; Peng, X. G. *J. Am. Chem. Soc.* **2001**, *123*, 183.
- (23) Yu, W. W.; Peng, X. G. *Angew. Chem., Int. Ed.* **2002**, *41*, 2368.
- (24) Reiss, P.; Bleuse, J.; Pron, A. *Nano Lett.* **2002**, *2*, 781.
- (25) Talapin, D. V.; Nelson, J. H.; Shevchenko, E. V.; Aloni, S.; Sadtler, B.; Alivisatos, A. P. *Nano Lett.* **2007**, *7*, 2951.
- (26) Reiss, P.; Protiere, M.; Li, L. *Small* **2009**, *5*, 154.
- (27) Hines, M. A.; Guyot-Sionnest, P. *J. Phys. Chem.* **1996**, *100*, 468.



- (28) Mattoussi, H.; Mauro, J. M.; Goldman, E. R.; Anderson, G. P.; Sundar, V. C.; Mikulec, F. V.; Bawendi, M. G. *J. Am. Chem. Soc.* **2000**, *122*, 12142.
- (29) Susumu, K.; Uyeda, H. T.; Medintz, I. L.; Pons, T.; Delehanty, J. B.; Mattoussi, H. *J. Am. Chem. Soc.* **2007**, *129*, 13987.
- (30) Liu, W.; Howarth, M.; Greytak, A. B.; Zheng, Y.; Nocera, D. G.; Ting, A. Y.; Bawendi, M. G. *J. Am. Chem. Soc.* **2008**, *130*, 1274.
- (31) Mei, B. C.; Susumu, K.; Medintz, I. L.; Delehanty, J. B.; Mountziaris, T. J.; Mattoussi, H. *J. Mater. Chem.* **2008**, *18*, 4949.
- (32) Susumu, K.; Mei, B. C.; Mattoussi, H. *Nat. Protoc.* **2009**, *4*, 424.
- (33) Lees, E. E.; Gunzburg, M. J.; Nguyen, T. L.; Howlett, G. J.; Rothacker, J.; Nice, E. C.; Clayton, A. H. A.; Mulvaney, P. *Nano Lett.* **2008**, *8*, 2883.
- (34) Jung, J. J.; Solanki, A.; Memoli, K. A.; Kamei, K.; Kim, H.; Drahl, M. A.; Williams, L. J.; Tseng, H. R.; Lee, K. *Angew. Chem., Int. Ed.* **2010**, *49*, 103.
- (35) Stewart, M. H.; Susumu, K.; Mei, B. C.; Medintz, I. L.; Delehanty, J. B.; Blanco-Canosa, J. B.; Dawson, P. E.; Mattoussi, H. *J. Am. Chem. Soc.* **2010**, *132*, 9804.
- (36) Uyeda, H. T.; Medintz, I. L.; Jaiswal, J. K.; Simon, S. M.; Mattoussi, H. *J. Am. Chem. Soc.* **2005**, *127*, 3870.
- (37) Li, Z.; Jin, R. C.; Mirkin, C. A.; Letsinger, R. L. *Nucleic Acids Res.* **2002**, *30*, 1558.
- (38) Park, J. S.; Vo, A. N.; Barriet, D.; Shon, Y. S.; Lee, T. R. *Langmuir* **2005**, *21*, 2902.
- (39) Srisombat, L. O.; Park, J. S.; Zhang, S.; Lee, T. R. *Langmuir* **2008**, *24*, 7750.
- (40) Zhang, S. S.; Leem, G.; Srisombat, L. O.; Lee, T. R. *J. Am. Chem. Soc.* **2008**, *130*, 113.
- (41) Gunsalus, I. C.; Barton, L. S.; Gruber, W. *J. Am. Chem. Soc.* **1956**, *78*, 1763.
- (42) Howie, J. K.; Houts, J. J.; Sawyer, D. T. *J. Am. Chem. Soc.* **1977**, *99*, 6323.
- (43) Bucher, G.; Lu, C. Y.; Sander, W. *ChemPhysChem* **2005**, *6*, 2607.
- (44) Cossi, M.; Rega, N.; Scalmani, G.; Barone, V. *J. Comput. Chem.* **2003**, *24*, 669.
- (45) Miertus, S.; Scrocco, E.; Tomasi, J. *Chem. Phys.* **1981**, *55*, 117.
- (46) Ji, X.; Palui, G.; Avellini, T.; Na, H. B.; Yi, C.; Knappenberger, K. L.; Mattoussi, H. *J. Am. Chem. Soc.* **2012**, *134*, 6006.
- (47) Amelia, M.; Font, M.; Credi, A. *Dalton Trans.* **2011**, *40*, 12083.
- (48) McLaurin, E. J.; Greytak, A. B.; Bawendi, M. G.; Nocera, D. G. *J. Am. Chem. Soc.* **2009**, *131*, 12994.
- (49) Grutzendler, J.; Yang, G.; Pan, F.; Parkhurst, C. N.; Gan, W. B. *Cold Spring Harb. Protoc.* **2011**, DOI: 10.1101/pdb.prot065474.
- (50) Yang, G.; Pan, F.; Parkhurst, C. N.; Grutzendler, J.; Gan, W. B. *Nat. Protoc.* **2010**, *5*, 201.
- (51) Choi, H. S.; Liu, W.; Misra, P.; Tanaka, E.; Zimmer, J. P.; Ipe, B. I.; Bawendi, M. G.; Frangioni, J. V. *Nat. Biotechnol.* **2007**, *25*, 1165.
- (52) Sandoval, R. M.; Molitoris, B. A. In *Methods in Molecular Biology*; Ivanov, A. I., Ed.; Humana Press, Inc., Totowa, NJ, 2008; Vol. 440, p 389.
- (53) Park, J.; Nam, J.; Won, N.; Jin, H.; Jung, S.; Jung, S.; Cho, S. H.; Kim, S. *Adv. Funct. Mater.* **2011**, *21*, 1558.
- (54) Clapp, A. R.; Goldman, E. R.; Mattoussi, H. *Nat. Protoc.* **2006**, *1*, 1258.